Triggers and signatures of shear banding in steady and time-dependent flows

S. M. Fielding
Department of Physics, Durham University, Science Laboratories, South Road, Durham, DH1 3LE, UK
(Dated: November 28, 2016)

This précis is aimed as a practical field-guide to situations in which shear banding might be expected in complex fluids subject to an applied shear flow. Separately for several of the most common flow protocols, it summarises the characteristic signatures in the measured bulk rheological signals that suggest the presence of banding in the underlying flow field. It does so both for a steady applied shear flow, and for the time-dependent protocols of shear startup, step stress, finite strain ramp, and large amplitude oscillatory shear. An important message is that banding might arise rather widely in flows with a strong enough time-dependence, even in fluids that do not support banding in a steadily applied shear flow. This suggests caution in comparing experimental data with theoretical calculations that assume a homogeneous shear flow. In a brief postlude, we also summarise criteria in similar spirit for the onset of necking in extensional filament stretching.

arXiv:1512.04715v2 [cond-mat.soft] 24 Nov 2016

I. INTRODUCTION

Many complex fluids show shear banding, in which a state of initially homogeneous shear flow becomes unstable to the formation of coexisting bands of differing shear rate, with layer normals in the flow-gradient direction. See the sketches inset in Fig. 1. (This précis concerns only this case of 'gradient banding'; for a discussion of 'vorticity banding', see [1, 2].) First observed in wormlike micellar surfactants in the mid 1990s [3], it has since also been seen in lyotropic lamellar phases [4], triblock copolymers [5], star polymers [6], carbopol gel [7], clays [8, 9], emulsions [9] and (subject to ongoing controversy [10, 11]) entangled monodisperse linear polymers [12, 13]. For reviews, see [2, 14–16].

To date, the majority of studies have focused on the case of steadily applied shear flow, with banding as the ultimate steady state response. However the last 5-10 years have seen a growing realisation that banding might also arise rather widely in flow protocols with a strong enough time-dependence, even in fluids that do not support banding in steady shear [16–24].

In startup of steady simple shearing flow ("shear startup"), for example, the (near ubiquitous) presence of an overshoot in the shear stress startup signal has been identified as a possible trigger for the formation of shear bands, at least transiently, en route to a steady flowing state [7, 13, 16–35]. A declining time-dependent viscosity has been similarly identified as a trigger for banding following the imposition of a step stress [16–18, 26, 27, 29, 36–40]. In these two protocols the time-dependence is transient, persisting typically for a few strain units as a steady flow is established out of an initial rest state. Accordingly, any bands must themselves be transient and heal back to homogeneous flow in the final steady state (unless the fluid also has banding as its ultimate steady state response). In soft 'glassy' materials with sluggish relaxation timescales, however, these startup bands might persist long enough to be mistaken for the ultimate flow response of the material for any practical purpose, despite being technically transient [16, 20].

Other flow protocols have sustained time-dependence: large amplitude oscillatory shear (LAOS) is a notable example [41]. In the mindset of the previous paragraph, one might intuitively view a strain-imposed LAOS experiment (hereafter abbreviated as LAOStrain), in some range of frequencies at least, as a repeating process of forward then backward startup runs. Any banding associated with the response of the same fluid to startup of steady shear flow might then be anticipated to recur in each half cycle of LAOS. Banding would then be an integral, sustained feature of LAOS, even if the fluid would not support banding in steadily applied shear [19, 42].

The aim of this précis is to summarise criteria for, and signatures of, the onset of banding, separately for each flow protocol [17]. It is offered as a field guide to situations in which banding might be expected in complex fluids and soft solids. An important by-product is also to suggest that banding might arise quite generically in flows with a strong enough time dependence, even in materials that don't support banding in steady state.

For each flow protocol in turn, we give a criterion [17] for the onset of banding in terms of a characteristic signature in the shape of the relevant bulk rheological response function for that protocol, *e.g.*, stress versus strain in shear startup. As a starting point for a hydrodynamic stability calculation, this response function is first calculated for a 'base state' in which the flow is assumed to stay homogeneous. A linear stability analysis then reveals the point at which this base state first becomes unstable to banding, and gives an onset criterion in terms of the functional shape of the response function associated with that base state. However because the flow is by definition homogeneous before it bands, these onset criteria can also be applied directly to the functional shape of the experimentally measured rheological response function. (This concept is explained more fully after (3) below.)

For anyone not wishing to read the rest of the paper, the signatures are summarised at a glance for steady applied shear flow in Figs. 1 and 2. The signatures for the transiently time-dependent flows of shear startup, step stress, and finite strain ramp are likewise summarised in Figs. 3, 4 and 5 respectively. For LAOS, with its sus-

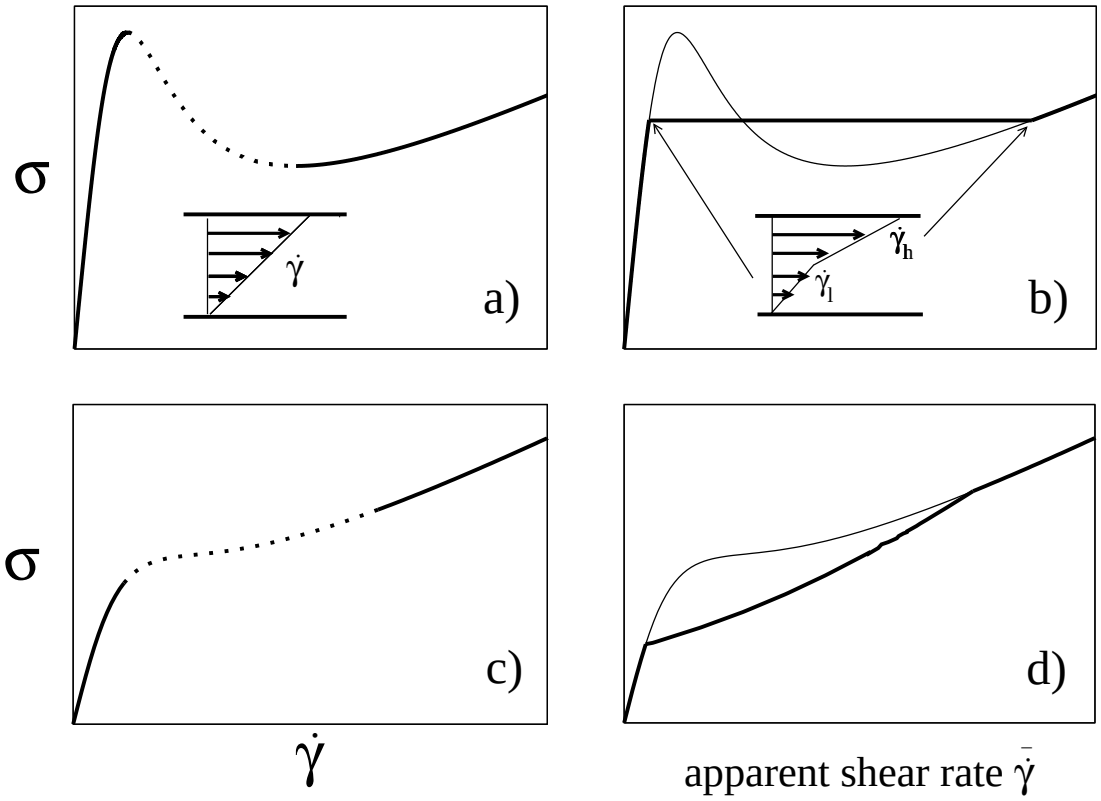

FIG. 1. Triggers and signatures of shear banding in a steadily applied shear flow. Left panels (a,c) show underlying constitutive relations between shear stress and shear rate, calculated within the assumption of a homogeneous shear flow. In (a), a state of initially homogeneous shear flow is linearly unstable, in the regime of negative constitutive slope, to the formation of shear bands. The steady state flow curve (b) then has a characteristic stress plateau in the shear banding regime. The presence of flow-concentration coupling would extend the window of linear instability in (a). It can also render a purely monotonic constitutive curve linearly unstable to banding, as shown in panel (c). The signature of concentration coupling in the ultimate banded state is then an upward slope in the stress 'plateau', as shown in panel (d). Line key: in the underlying constitutive curves (a) and (c) the thick solid lines denote homogeneous flow states that are linearly (though not necessarily absolutely) stable against shear banding, while the thick dotted lines denote homogeneous flow states that are linearly unstable to the formation of shear bands. In the flow curves (b) and (d) the thick solid lines represent steady flowing states (which are shear banded in some regimes as described above) while the thin solid lines represent the underlying constitutive curves, copied from (a) and (c).

tained time-dependence, we sketch in Fig. 6 the regions of the plane of applied strain rate amplitude and cycle frequency in which banding is anticipated.

Once significant banding develops, it in general changes the shape of the response function compared to that calculated within the assumption of homogeneous flow. This provides a note of caution to the endeavour of benchmarking new constitutive models by comparing homogeneous calculations with experiment in any of the widespread situations where banding might arise.

Most theoretical work to date in this area has been on models of linear entangled polymeric fluids (polymer solutions and melts, and wormlike micelles) [17, 18]; and of soft 'glassy' materials (foams, dense emulsions, dense colloids, microgels, *etc.*) [16, 20–23], which typically show a yield stress and rheological aging. However it is hoped that the criteria might apply universally. These two classes are exemplary only, and were selected for study because they are the most familiar to this author. Indeed this précis is highly selective and focused mainly on the author's own work. Work by others to further generalise, or delineate the regimes of applicability of these criteria would be very welcome.

II. SHEAR BANDING IN STEADY IMPOSED FLOWS

We consider first the long-time response of a fluid to a steadily applied shear flow. In the interests of definite vocabulary, we shall use the term "constitutive curve" to denote a material's underlying stationary relation $\sigma(\dot{\gamma})$

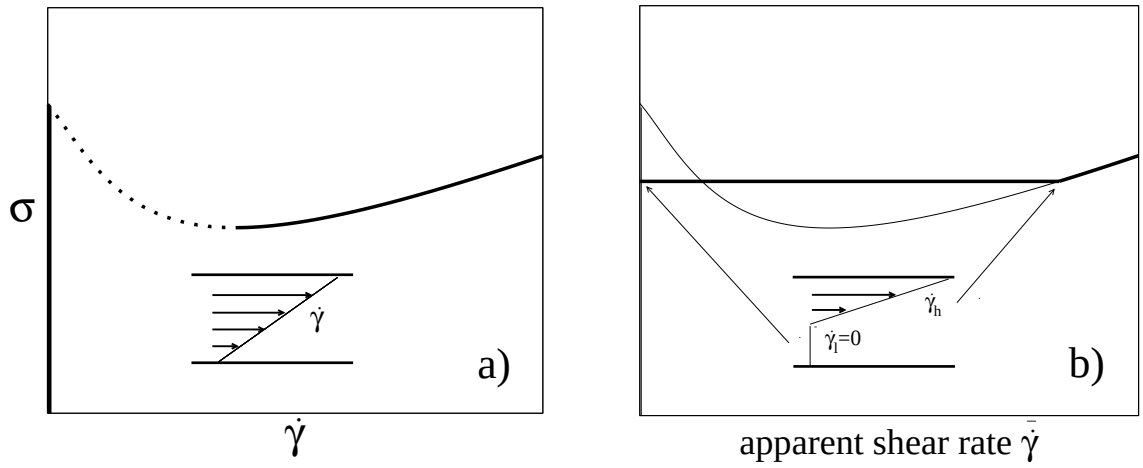

FIG. 2. Triggers and signatures of shear banding in a steadily applied shear flow in a yield stress fluid. Left panel (a) shows an underlying constitutive relation between shear stress and shear rate, calculated within the assumption of a homogeneous shear flow. A state of initially homogeneous shear flow is linearly unstable in the regime of negative constitutive slope to the formation of shear bands. The steady state flow curve (b) then has a characteristic stress plateau in the shear banding regime. Compared with the corresponding sketch for ergodic fluids in Fig. 1, the low-shear branch of the constitutive curve lies vertically up the stress axis in (a) and the corresponding band in (b) is unsheared. (As discussed in the text, concentration coupling is also possible in these yield stress materials, but we have not sketched it separately.) Line key: as in Fig. 1.

between shear stress and shear rate, calculated within the assumption that the flow remains spatially uniform with the shear rate everywhere equal to $\dot{\gamma}$. Although stationary, however, states on this curve may not be stable against banding. Where shear bands form, we term the steady state relation between shear stress and shear rate the composite "flow curve", with the relevant shear rate now being the spatially averaged value across the cell, *i.e.*, the relative wall velocity normalised by the gap size, often termed the "apparent shear rate". In the absence of banding, these two curves coincide.

A. Steady state bands

A state of initially homogeneous shear flow is known to be linearly unstable in any regime where the fluid's underlying constitutive curve has negative slope [43]:

$$\frac{d\sigma}{d\dot{\gamma}} < 0. \tag{1}$$

See Fig. 1a. Shear bands then form, and the steady state composite flow curve displays a characteristically flat plateau [44], Fig. 1b. In a curved flow cell, this plateau will in fact have a slight positive slope [45]. (Indeed, taking into account intrinsic heterogeneity in the flow field due to device curvature is an important step in benchmarking constitutive models, even in the absence of true banding.) In the windows of shear rate within the steady state banding regime, but either side of the linearly unstable regime, an initially homogeneous flow is metastable to banding [46]. In this regime, in a slow strain rate sweep at least, a finite amplitude perturbation to an initially homogeneous flow is required to initiate banding. Possible sources include initial heterogeneities following sample preparation, mechanical noise in the rheometer, or true thermal noise. (In a shear startup at such shear rates, a linear instability can arise during that time-dependent startup process. However we defer further discussion of these time-dependent phenomena to Sec. III A below.)

In two-component viscoelastic fluids (solutions), spatial variations in the flow field are in general dynamically coupled to variations in the concentration field ϕ [47–54]. This provides a positive feedback mechanism that enhances a fluid's tendency to form shear bands [55–57], giving a modified onset criterion of the general form

$$\frac{d\sigma}{d\dot{\gamma}} + C_{\dot{\gamma}\phi} < 0. \tag{2}$$

In this inequality, $C_{\dot{\gamma}\phi}$ is a flow-concentration coupling term. Its full form is given in Eqn. (4.20) of Ref. [55] and is rather complicated. However in essence its numerator comprises the derivative of shear stress with respect to concentration, multiplied by the derivative of a normal stress-like variable with respect to shear rate. Its denominator comprises (in essence) the (bare) osmotic modulus minus the derivative of a normal stress-like variable with respect to concentration. The overall effect of this coupling is such that the regime in which an initially homogeneous flow is predicted to be linearly unstable to the formation of shear bands extends slightly beyond the dotted region in Fig. 1a).

More importantly, flow-concentration coupling can also render a weakly sloping but monotonic constitutive curve unstable to banding. See Fig. 1c). This was first explored in the context of polymeric fluids [55–57]. It has recently been studied again in polymers [58, 59], and also applied to yield stress colloidal fluids [60, 61]. The signature of concentration coupling in the steady state composite flow curve is an upward slope in the 'plateau' of the banding regime. For strong coupling this can be quite pronounced, as sketched in Fig. 1d). For weak coupling it may go unnoticed.

The sketches in Figs. 1 pertain to ergodic fluids with fixed, finite stress relaxation timescales. However shear banding also arises widely in non-ergodic soft glassy materials [16], which have a yield stress σ_Y associated with sluggish and often aging stress relaxation timescales. (Throughout we use the term yield stress to denote the limiting shear stress obtained as $\dot{\gamma} \to 0$ in a slow strain rate sweep down the flow curve.) In this case the constitutive curve's high viscosity branch lies vertically up the σ axis, as sketched in Fig. 2. The band associated with this branch is then unsheared, and coexists with a flowing band of non-zero shear rate on the other flow branch [9, 62], as sketched in the inset to Fig. 2b). Otherwise, the comments of this section generally apply.

B. Oscillatory and chaotic shear bands

The discussion so far has assumed that a fluid's ultimate response to a steadily applied shear will be a state of steady flow. In some cases, however, oscillations or even chaotic fluctuations can arise [63, 64]: not transiently, but as the ultimate response of the material, sustained as long as the flow remains applied. Spatio-temporally oscillating and chaotic shear bands were explored in Refs. [65–67]. We do not discuss them further here.

III. SHEAR BANDING IN TRANSIENTLY TIME-DEPENDENT FLOWS

We now turn to protocols in which the applied flow is itself inherently time-dependent. In this section we consider situations in which that time-dependence is transient in nature: arising either during a process whereby a steady flow is established out of an initial rest state (in shear startup or following the imposition of a step stress), or after a finite strain ramp as the system relaxes back to equilibrium. For the remainder of this précis we ignore concentration coupling, deferring to future work a study of its effects in time-dependent flows.

A. Shear startup

A common flow protocol consists of taking a sample that is initially at rest and with any residual stresses well relaxed, then at some time $t = 0$ suddenly jumping the strain rate to some value $\dot{\gamma}$ that is held constant thereafter. Measured in response to this is the shear stress startup signal $\sigma(t)$ as a function of the time t (or accumulated strain $\gamma = \dot{\gamma}t$) since the inception of the flow. This typically evolves as sketched in Fig. 3, with an initial regime of linear elastic response in which the stress rises proportionally with the strain, followed by an overshoot at a strain $\gamma = O(1)$, then a final decline to a steady state value on the flow curve at the given strain rate.

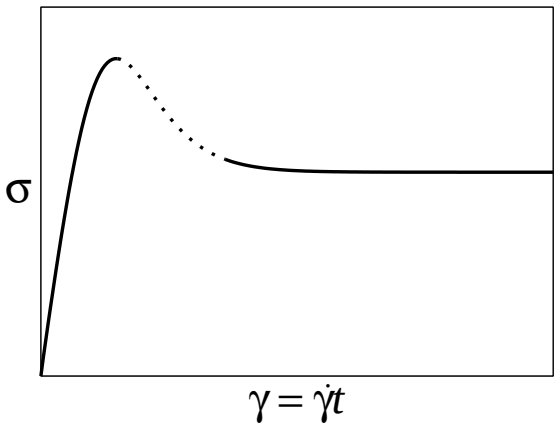

FIG. 3. Typical shear stress response in shear startup. The region of linear instability to the formation of shear bands is sketched as dotted. Depending whether the same fluid also supports steady state bands at the flow rate in question, according to the sketches in Fig. 1, these startup bands either persist to steady state or heal back to homogeneous flow. (In the former case, the line should be dotted even at long times.)

In Ref. [17], it was argued that the presence of an overshoot in this startup signal is generically indicative of a strong tendency to form shear bands, at least transiently during the startup process. Accordingly – though in sketch form only (we discuss corrections and caveats below) – the criterion for the onset of banding in startup is

$$\frac{d\sigma}{d\gamma} < 0, \tag{3}$$

as indicated by the dotted line in Fig. 3.

This criterion (3) was derived by first calculating the stress signal associated with an underlying time-evolving homogeneous base state startup flow, artificially imposing (for the purposes of that preliminary calculation) the constraint that the flow must remain homogeneous. Performing a linear stability analysis for the dynamics of heterogeneous fluctuations about this time-evolving base state then shows that it first becomes unstable to the formation of shear bands just after the stress overshoot. In this way, an overshoot in the startup signal associated with that underlying time-evolving base state is predicted to act as a trigger to banding. These considerations can then be applied to real data by recognising that before

any banding arises in any given experiment, the flow is (by definition) homogeneous and so accords with the base state of the homogeneous calculation. We thus recognise that the criterion (3) can also be applied directly to the experimentally measured stress startup signal.

A common misconception is that it is instead the onset of banding that causes the stress drop. While it is true that once significant banding develops it in general reduces the stress compared to that calculated assuming homogeneity, thereby accentuating the drop, the primary direction of causality (at least in all the models this author has studied to date) is the opposite: the onset of banding is triggered by the stress drop, not vice versa.

As noted above, this discrepancy between the stress signal of the homogeneous base state and that of the full shear banded flow should provide a note of caution to the common practice of benchmarking new constitutive models by comparing experimental startup data with calculations that assume the flow to remain homogeneous.

In any fluid for which the ultimate constitutive response also admits steady state banding as in Sec. II A above, these bands that form during startup will persist to steady state. In fluids that don't support steady state banding, the startup bands instead heal back to homogeneous shear. Indeed, in this case the tendency to form bands persists only transiently. With this in mind, it is important to note that not only must condition (3) be satisfied, but the banding instability must also be strong enough for long enough to ensure that observable banding can develop before homogeneous flow is recovered. Clearly, a more pronounced stress overshoot is more likely to give rise to more strongly observable banding.

Despite technically being transient, however, in soft glasses with sluggish relaxation timescales, the bands may persist long enough to be mistaken for the ultimate flow response of the material [16, 20]. Soft glasses are also predicted to exhibit a strong age dependence: a sample that is older and more solid-like before the flow commences shows a stronger overshoot [30, 68–71], and is predicted to show more pronounced startup bands [16, 20].

Intuitively, then, the startup banding just described is triggered as the material 'yields' and starts to flow, post-overshoot. However it is important to note that while the stress drop and associated banding may indeed arise from actual yielding, *i.e.*, increasing plasticity, as in a soft glass [16, 20], it can equally stem from falling elasticity. The latter scenario is predicted [17–19, 24] by the Rolie-poly model [72] of linear polymers at shear rates exceeding the inverse reptation time τ_d but less than the inverse chain stretch relaxation time τ_R. (A small correction to (3) in this context is however discussed below.) In this regime the stress startup curve is a unique function of strain, independent of strain rate, but nonetheless sufficiently nonlinear to show an overshoot. Although the coincidence of the criterion (declining stress as a function of accumulated strain) for banding instability in both these scenarios of plastic yielding and falling-elasticity is highly suggestive of common physics, further work is needed to elucidate this fully.

Evidence to date for banding associated with stress overshoot in startup can be summarised as follows. It has been seen experimentally in polymeric fluids including wormlike micelles [25, 26] and linear polymers [13, 27–29]; and in soft glassy materials including carbopol gel [7, 30], Laponite clay [31, 73], a non-Brownian fused silica suspension [35] and waxy crude oil [71]. Molecular simulations have captured it in polymers [32, 74], a model colloidal gel [75] and molecular glasses [33, 76, 77]. A model foam displayed it in [78, 79]. Linear stability analysis and nonlinear simulations predict it in the Rolie-poly model of polymers [17–19, 24], the soft glassy rheology (SGR) and fluidity models of soft glasses [16, 20, 80], the STZ model of amorphous elastoplastic solids [21, 22, 81], a mesoscopic model of plasticity [23], and a model of polymer glasses [34]

With the aim of providing a unified understanding of all these observations, a theoretical criterion for the onset of banding in startup was derived analytically in Ref. [17] on the basis of a constitutive model written in a highly generalised, though still differential, form. It was shown to indeed be closely associated with stress overshoot, consistent with the evidence summarised in the previous paragraph. It also showed full quantitative agreement with numerical calculations in the Rolie-poly model [18].

However to make progress analytically the calculation allowed for only two viscoelastic variables: the viscoelastic shear stress σ_v and one component of normal stress n. Specifically, for this case of simple shear flow it considers a force balance condition for a total shear stress $\sigma = \sigma_v + \eta\dot{\gamma}$ comprising a viscoelastic contribution σ_v and a Newtonian solvent stress $\eta\dot{\gamma}$. Generalised constitutive dynamics for the viscoelastic stresses are then prescribed as $\dot{\sigma_v} = f(\dot{\gamma}, \sigma_v, n)$ with $\dot{n} = g(\dot{\gamma}, \sigma_v, n)$, with n a normal stress variable. The functions f and g are left unspecified in the interests of generality, but include stress relaxation on a timescale τ. More generally still, however, more viscoelastic variables besides σ_v and n should be included (as will usually arise after extracting componentwise equations for a fully tensorial constitutive model in shear). Examples include the second normal stress (even in a single mode description); or contributions to the stress from additional modes with faster relaxation times.

Accordingly, the status of (3) more generally remains unclear: it does not appear to apply in a straightforward way in the Giesekus model, for example [18]. However (3) does correctly predict the onset of banding instability during startup in the Rolie-poly model [18] (with a small correction discussed below) and in models of soft glasses [16, 20], including the SGR model (which, being of integral form, effectively has infinitely many viscoelastic modes); and accords well with the evidence from experiment and molecular simulation described above.

Taken together, then, the evidence to date for banding triggered by overshoot appears widespread and quite convincing. It suggests that experimentalists should be alert

to possible banding in any startup experiment where the stress signal shows a strong overshoot; and that theorists should exercise caution in benchmarking homogeneous calculations against experiment.

As just described, the criterion derived in Ref. [17] is closely associated with the overshoot in the stress startup curve, as written in (3). In fact, the full formula (Eqn. 20 in the Supplementary Material of Ref. [17]) contains not only the slope of the stress with respect to strain, but also a smaller correction term involving the curvature: the instability technically first sets in just before overshoot, as the stress signal curves down after the initial regime of linear elasticity. This agrees fully with numerics in the Rolie-poly model [18], though in practical terms only modest bands with weakly differentiated shear rates arise before the overshoot.

The discussion in this section has focused on a single startup experiment in which the shear rate is discontinuously jumped from zero to some constant value. Similar effects have also been explored experimentally [82] in fast upward shear rate sweeps in soft glasses.

B. Step stress

We consider now a previously undisturbed sample subject at some time $t = 0$ to the imposition of a shear stress that is held constant thereafter. Typically measured in response to this is the creep curve $\gamma(t)$, often reported as its time-differential $\dot{\gamma}(t)$. In many cases this shows an initial regime of slow creep in which the strain rate progressively declines, followed by a more rapid yielding process in which the strain rate increases to attain its final steady state on the flow curve. See Fig. 4.

In [17], it was shown that the criterion for instability to banding is that this differentiated creep curve obeys:

$$\frac{d^2\dot{\gamma}}{dt^2} / \frac{d\dot{\gamma}}{dt} > 0. \tag{4}$$

A material is therefore predicted to be unstable to forming shear bands, at least transiently, if its differentiated creep curve simultaneously slopes upward and curves upward as a function of time. See the dotted regime in Fig. 4. (Simultaneous downward slope and curvature are also predicted to initiate banding, but this author does not know of any instances of such response.)

As in shear startup discussed above, this criterion is derived by first calculating the creep response of an underlying base state in which the sample is assumed to remain homogeneous, then performing a linear stability analysis to determine the condition under which that base state first becomes unstable to banding. And, by arguments analogous to those just after (3), because the flow is by definition homogeneous before it bands, (4) can also be applied to the experimentally measured creep curve.

As in shear startup, then, banding is predicted to arise as the material starts to 'yield' towards a flowing state after a regime of initially more solid-like response. In the models of polymeric fluids that this author has studied to date, such a scenario arises to most pronounced effect at imposed stresses just above the local maximum in a nonmonotonic constitutive curve of the form in Fig. 1a), or in the region of weak positive slope in a monotonic curve as in Fig. 1c) [18]. In the soft glassy rheology model, which has a monotonic constitutive curve, it arises most strongly for imposed stresses just above the yield stress [16, 17], and is more pronounced in a sample aged into a more solid-like state before the stress is applied.

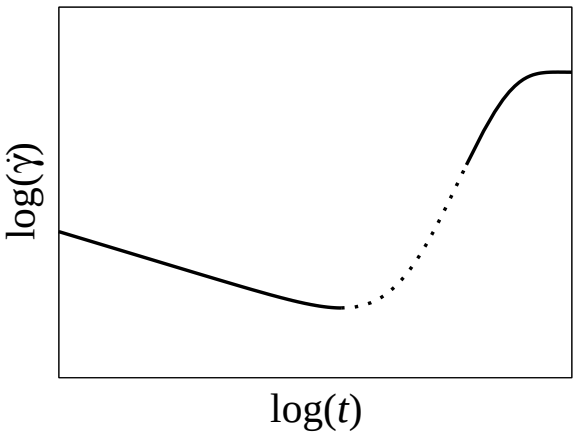

FIG. 4. Typical evolution of the time-differentiated creep response curve following the imposition of a step stress. The regime of linear instability to banding is shown as dotted.

In all cases studied to date these bands heal back to homogeneous flow in the ultimate steady state, consistent with the fact that steady state banding can only be accessed under conditions of imposed strain rate. (Recall that the flow curve is a flat function of strain rate in the banding regime, at least in the absence of concentration coupling.) In soft glasses with sluggish relaxation times, however, they can persist a very long time, particularly for initially well aged samples subject to imposed stresses only just exceeding the yield stress [16, 17].

Evidence to date for banding after a step stress can be summarised as follows. It has been seen experimentally in polymers [27, 29, 38], wormlike micelles [26, 36, 37], carbopol gel [39, 83], carbon black [40, 84] and a colloidal glass [85]. Particle based simulations of molecular glasses have captured it [86]. Linear stability calculations and direct numerical simulations have demonstrated it in the Rolie-poly and Giesekus models of polymers [18], though as a weaker effect in the latter model. Stochastic simulations have confirmed it as a strong, age-dependent phenomenon for imposed stresses just above the yield stress in the soft glassy rheology (SGR) model [16, 17].

More universally, the criterion (4) was derived within a constitutive model written in highly general, though still differential form [17]. In contrast to its counterpart (3) for startup, which is subject to the caveat discussed in the previous section, the derivation of (4) placed no

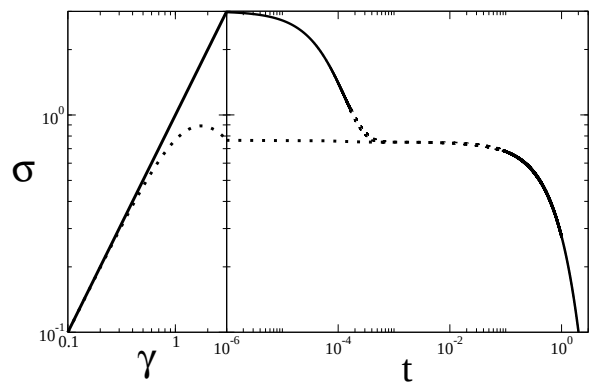

FIG. 5. Typical evolution of the shear stress with strain during a rapid strain ramp, then decay of the stress as a function of the time post-ramp. Regimes of linear instability to banding are sketched as dotted. Data taken from calculations performed with the Rolie-poly model [18].

limitations on the number of dynamic viscoelastic variables present in the constitutive description. Accordingly it should even apply to constitutive models of integral form (which can be cast in differential form with infinitely many dynamical variables). This is consistent with the observation of banding following a step stress in the SGR model, which indeed has a constitutive equation of integral form [16, 17].

On the basis of the evidence just summarised, we suggest that the criterion (4) for instability to shear banding following the imposition of a step stress might apply universally to all materials.

C. Rapid finite strain ramp

We now turn to the protocol that is sometimes called 'step strain', but is in practice a fast finite strain ramp: a previously undisturbed material is subject after some time $t = 0$ to a linearly increasing strain $\gamma = \dot{\gamma}t$. Once some accumulated strain γ_0 is reached the strain rate is set to zero, and the strain remains constant at $\gamma = \gamma_0$. Measured in response is the stress as a function of the time (or accumulated strain) during the ramp itself, then the stress decay as a function of time as the system relaxes back to equilibrium post-ramp. See Fig. 5.

During the ramp itself, the stability properties of an initially homogeneous base state to the onset of banding are the same as in shear startup, because the two protocols are the same in this regime. However we focus here on ramps that most closely approximate the notion of a 'step strain', and are therefore sufficiently fast that no meaningful banding has time to develop during the ramp (even if a homogeneous shear is technically unstable to banding during it). Our interest is instead in whether any appreciable banding arises during the stress relaxation post-ramp.

In Ref. [17] we showed that a state of initially homogeneous shear will be unstable towards starting to form bands after the ramp ends if the stress as a function of accumulated strain just *before* the ramp ended had negative slope. See the dotted line in the left part of Fig. 5. In other words, criterion (3) applies, interpreted in the manner just discussed. (Caveats about the number of dynamical variables in the generalised constitutive model used to derive the criterion do not apply post ramp. Other, milder assumptions are discussed in Ref. [17, 18].)

Numerical studies of the Rolie-poly model of polymers and wormlike micelles are consistent with this prediction [18, 19, 87]. For a ramp rate $\dot{\gamma}$ in the range $1/\tau_d < \dot{\gamma} < 1/\tau_R$, the stress shows an overshoot during the ramp at a critical strain of $O(1)$. Provided this strain is exceeded, instability to banding will ensue post-ramp. See the lower curve in Fig. 5. In contrast, for ramp rates $\dot{\gamma} > 1/\tau_R$ the development of chain stretch causes linear elastic response during the ramp itself, stabilising the system against banding immediately post-ramp. See the upper curve in Fig. 5. However, that stabilising stress then quickly decays on a timescale of $O(\tau_R)$, leaving the sample in a state as if no stretch had developed in the first place, and therefore susceptible to banding. (In fact, that is only true if an effect known as 'convective constraint release' [88, 89] is not too strong.) The Rolie-poly model thus predicts transient banding as the sample relaxes back to equilibrium after a rapid strain ramp. This is consistent with early theoretical intuition [90], and with experimental observations in polymers [91–98] and wormlike micelles [36].

In the SGR and fluidity models of soft glasses, the stress rises linearly during a fast strain ramp and decays relatively slowly after it: (3) is not satisfied, and no banding is predicted. (This is however still consistent with the prediction of banding in shear startup at more modest flow rates, as discussed in Sec. III A above.) Indeed, this author does not know of any experimental observations of banding after step strain in soft glasses.

IV. BANDING IN PERPETUALLY TIME-DEPENDENT FLOWS

We turn now to an imposed flow that is perpetually time-dependent: large amplitude oscillatory shear (LAOS) [41]. Our remarks here will be brief: a longer manuscript by this author and coworkers has been submitted to the same issue of this journal [42].

We focus mainly on LAOStrain with an imposed strain rate $\dot{\gamma}(t) = \gamma_0\omega\cos(\omega t) = \dot{\gamma}_0\cos(\omega t)$, such that any given experimental run is prescribed by the strain rate amplitude $\dot{\gamma}_0$ and cycle-frequency ω, or equivalently the strain amplitude γ_0 and ω. (Expressed in units of the fluid's inverse intrinsic relaxation time, $\dot{\gamma}_0$ and ω are often respectively termed the Weissenberg and Deborah number.) Typically, after many cycles a pseudo-steady state (often called an "alternance state") is attained in

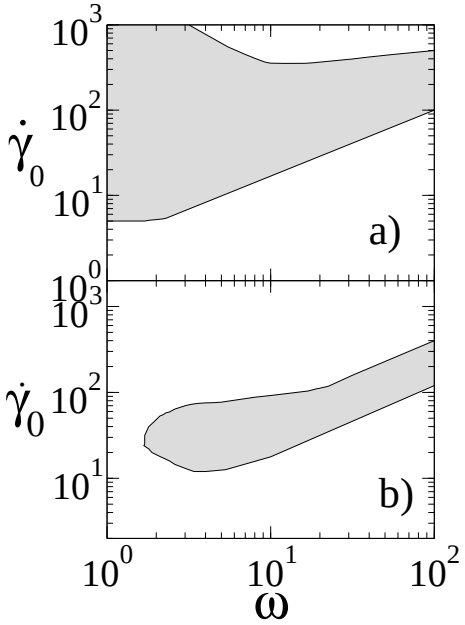

FIG. 6. Shear banding in LAOStrain. Shaded areas indicate the regimes of shear rate amplitude $\dot{\gamma}_0$ and cycle frequency ω in which shear banding might be expected in a LAOStrain experiment with an imposed strain rate $\dot{\gamma}(t) = \dot{\gamma}_0 \cos(\omega t)$, for a polymeric fluid with a non-monotonic underlying constitutive curve (panel a) and a monotonic constitutive curve (panel b). Data are taken from calculations in the Rolie-poly model of polymeric fluids [42].

which the fluid's response is invariant from cycle to cycle, $t \to t + 2n\pi/\omega$. We focus on that regime, discarding any earlier cycles in which the response is still settling to the flow. Our aim is to understand in what regimes of applied $\dot{\gamma}_0$ and ω banding might arise, and to sketch these in the plane of $\dot{\gamma}_0, \omega$, noting that any coordinate pair in this plane refers to a single LAOS experiment at the given amplitude and frequency. To do so, it is helpful to consider first the dynamics of an underlying base state flow that is (artificially) assumed to remain homogeneous.

In a LAOS experiment performed at a low frequency $\omega \to 0$, the fluid will slowly explore its underlying stationary constitutive curve as the strain rate sweeps progressively up and down (over both positive and negative values) during a cycle. In this way, the so-called viscous Lissajous-Bowditch curve (*i.e.,* the stress signal plotted parametrically as a function of strain rate round the cycle) is expected to have the same form as the fluid's underlying constitutive curve (Fig. 1a,c). If this is non-monotonic, shear banding might then be expected in any low-frequency LAOS experiment that has a strain rate amplitude $\dot{\gamma}_0 = \gamma_0 \omega$ sufficiently large to enter the banding regime, according to the criterion (1) for banding in steady shear.

At higher frequencies we might instead expect a LAOStrain experiment to (loosely) correspond to a repeating sequence of forward and backward shear startup runs. In any LAOS experiment of sufficiently large strain amplitude γ_0, the elastic Lissajous-Bowditch curve of stress plotted parametrically as a function of strain might then be expected to show overshoots reminiscent of those in the stress startup curve associated with a single startup run. These overshoots might further be expected to trigger banding in each half of the cycle, according to a criterion resembling (3) for banding in startup. This should hold whether or not the stationary constitutive curve that determines the fluid's response to a steady flow (or a low-frequency LAOS run) is non-monotonic or monotonic.

This intuition was confirmed numerically in the Rolie-poly model of polymers and wormlike micelles in Ref. [19, 42]. The region of the $\dot{\gamma}_0, \omega$ plane in which shear banding was found is sketched in Fig. 6a) for a fluid with a non-monotonic constitutive curve. This shows banding at low frequency $\omega \to 0$, consistent with the fact that such a fluid also supports banding in steady shear flow. It also shows banding at high frequencies, reminiscent of banding in a fast shear startup, in each half cycle of the elastic Lissajous-Bowditch curve. For a fluid with a monotonic constitutive curve (Fig. 6b) the regime of low frequency banding is absent, as expected. Importantly, however, the regime of high frequency banding remains. In both Figs. 6a and b this regime of banding eventually closes off at very high ω once the solvent stress swamps the polymer contribution. (Data not shown.)

A thorough study of the effects of model parameter values was conducted in Ref. [42]. As expected, a stronger tendency to banding, over larger regions of the $\dot{\gamma}_0, \omega$ plane, was found for decreasing values of solvent viscosity η, decreasing levels of convective constraint release, and increasing entanglement number. Indeed, moving these parameter values too far in the opposite direction

can eliminate banding. This is to be expected: a large Newtonian viscosity swamps nonlinear viscoelasticity, for example.

While the details of Figs. 6a,b) are likely to be model dependent, these findings could have wider significance in suggesting that banding might arise quite generically in flows with a strong enough sustained time-dependence, even in fluids that do not support bands in steady flow.

Depending on the degree of shear banding that arises, the Lissajous-Bowditch curves of the banded flow state can differ quite significantly from those of the base state calculated within the assumption of a homogeneous flow. Indeed, in some cases shear bands can persist around the entire cycle. This should lend caution to attempts to develop rheological fingerprints within theoretical calculations that assume the flow to remain homogeneous. Theoretical studies that do account for banding in LAOStrain can be found in Refs. [19, 42, 99, 100].

As explored further in Ref. [42], shear banding is also predicted to arise in polymers subject to LAOStress.

Our discussion of LAOS has so far concerned ergodic fluids such as polymers and wormlike micelles, with finite stress relaxation timescales. Work by Rangarajan Radhakrishnan with this author concerning LAOStrain in the SGR model of soft glasses is also currently under review. As noted above, this model has a yield stress and a constitutive curve that rises monotonically beyond it, precluding true steady state banding. In view of this, and the preceding discussion, we might likewise expect the SGR model to respond homogeneously to an imposed LAOStrain experiment at low frequency $\omega \to 0$.

However the SGR model also displays rheological aging: in the absence of flow its stress relaxation timescales increase as a function of the sample age. An applied flow can then halt aging and restore an effective sample age set by the inverse flow rate. As a result, the response of the SGR model to a low frequency LAOStrain comprises a complicated sequence of processes in which it alternately ages into a solid-like state during the low shear phase of the cycle, then yields via a stress overshoot and associated banding in the high shear phase. In retrospect this is not surprising: an aging material has no characteristic relaxation timescale against which to compare the frequency ω of the applied flow. In view of this, and more broadly, shear banding may prove an integral feature of the response of soft glassy materials to imposed flows of arbitrarily slow time variation, even in the absence of true zero-frequency banding.

Experimentally, shear banding has been observed during LAOS in polymer solutions [91, 101], dense colloids [102], carbon black gels [103, 104], foams [105], non Brownian PMMA suspensions [106] and also in wormlike micellar surfactants that are known to shear band in steady state [107–109].

V. CONCLUSIONS

In this précis we have summarised criteria for shear banding in steady and time-dependent flows of complex fluids and soft solids. These criteria were derived analytically within a constitutive model written in a highly generalised (though still differential) form, and are supported by experimental observations, particle based simulations, linear stability analysis and numerical solutions of several widely used constitutive models in the exemplary contexts of polymeric fluids (polymers and wormlike micelles) and soft glassy materials (dense emulsions, dense colloids, microgels, *etc.*). While the evidence supporting the picture presented here is therefore quite convincing, we nonetheless now consider any caveats and uncertainties that remain.

Our most important caveat concerns the generality of the stress overshoot criterion for banding in shear startup. Although indeed derived in a constitutive model written in a generalised form, to make progress analytically this allowed for only two dynamical viscoelastic variables. As things stand, the status of the criterion more generally is not completely clear. For example, it appears not to apply in a straightforward way in the phenomenological Giesekus model of polymers. It does, though, convincingly hold in the Rolie-poly model of polymers, and in the fluidity and SGR models of soft glasses. Its verification in the SGR model seems an important result in this context, because that model's constitutive equation is of integral form, and so effectively has infinitely many dynamical variables. Nonetheless, future work would be welcome to try to generalise the criterion further, and to delineate more fully its regimes of applicability.

The criteria put forward for the other time-dependent protocols (step stress and during the stress relaxation following a fast strain ramp) are not subject to any limitations concerning the number of dynamical variables. Milder assumptions made in their derivations are discussed in the original papers [17, 18].

While the criteria presented predict the onset of an instability to the formation of bands, that instability must obviously be strong enough and persist for long enough in any time-dependent protocol to ensure that observable bands arise before the homogeneous base state regains stability. (Put more technically: instability is characterised in the calculation by a positive eigenvalue, which must remain positive and of large enough amplitude for long enough to ensure noticeable banding [24].) Clearly, for the example of startup, stronger stress overshoots are more likely to give observable banding. Weaker ones instead give transient instability and enhanced spatial fluctuations, but without leading to macroscopically observable bands (consistent with the absence of banding altogether in the regime of slow startup flows where overshoots are absent).

Our calculations to date have assumed the inertialess limit of creeping flow. In this limit, the eigenvector gov-

erning the onset of shear rate heterogeneity $\delta\dot{\gamma}$ has the form $\delta\dot{\gamma} = -\delta\sigma_v/\eta$ where σ_v is the shear component of the viscoelastic stress, and η is the viscosity of the background Newtonian solvent, and/or any viscoelastic modes fast enough not to be ascribed their own dynamical evolution. For most materials this background viscosity is very small, predicting a strong degree of heterogeneity in the flow field, $\delta\dot{\gamma}$, compared to that in the viscoelastic stress, $\delta\sigma_v$. This predicts potentially rather violent banding that may, ultimately, be tempered by inertia. While order of magnitude estimates suggest this should not be an important effect, concrete calculations are in progress to check this in more detail.

In polymeric fluids, numerical studies have so far mainly focused on the Rolie-poly model [72]. This is microscopically sophisticated enough to incorporate the dynamical processes of reptation, chain stretch, and convective constraint release, while also being simple enough to allow numerical progress. However it contains only a single reptation mode and a single stretch relaxation mode. Work is in progress to check the effects of multiple relaxation modes, in unbreakable polymers, on the effects discussed. In wormlike micelles (which are sometimes called "living polymers" due to their reversible breakage and recombination dynamics) a single mode description should already capture most of the physics (because breaking narrows the relaxation spectrum). Indeed, it would be interesting to perform a comprehensive study of time-dependent flows in wormlike micelles over the full phase diagram of concentration, including regimes of both non-monotonic and monotonic underlying constitutive curves.

Finally, although the effects of flow-concentration coupling are well understood in situations of steady state banding [55–57], their role in the time-dependent phenomena discussed above remains to be clarified.

The author hopes that this précis will provide a helpful guide to situations in which shear banding might be expected in complex fluids and soft solids subject to steady and time-dependent flows. Future work by other authors would be welcome to verify the criteria suggested here, to generalise them further, and/or to delineate any regimes in which they might break down. This seems particularly important for the case of shear startup, where it has been more difficult than in other protocols to obtain a universal criterion free of some caveats.

VI. POSTLUDE: CRITERIA FOR NECKING IN EXTENSIONAL FILAMENT STRETCHING

This section summarises work by David Hoyle with this author currently under review at the Journal of Rheology, in manuscripts "Criteria for extensional necking in complex fluids and soft solids: imposed Hencky strain rate protocols" and "Criteria for extensional necking in complex fluids and soft solids: imposed tensile stress and force protocols".

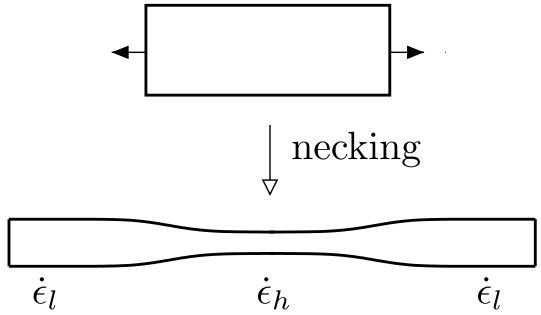

FIG. 7. Sketch of necking in extensional filament stretching. A cylindrical filament is seen here side-on.

Having focused on shear flow so far, we now conclude with a brief postlude concerning extensional flows. In particular we consider the phenomenon of necking in a cylindrical filament (or planar sheet) subject to stretching, as sketched in Fig. 7. Here a state of initially homogeneous flow, in which the filament is extending and thinning in a uniform way along its length, gives way to a heterogeneous state with a higher extension rate and more pronounced thinning in some part of the sample. A comparison between the sketches in Figs. 1 and 7 suggests an analogy between shear banding and extensional necking: the relevant deformation field (shear rate in Fig. 1 and extension rate in Fig. 7) becomes heterogeneous in both cases.

With that analogy in mind, in Refs. [110, 111], together with the manuscripts with Hoyle under review, we developed criteria for the onset of necking, separately for the flow protocols of step tensile stress, step tensile force, and startup of constant Hencky strain rate. As before, these were derived by studying the linearised dynamics of small heterogeneous perturbations, which are the precursors of a neck, about a state of initially homogeneous extensional flow. Also as before, they are expressed in terms of characteristic signatures in the shapes of the relevant underlying rheological response function for the given protocol. We now briefly summarise them, referring the reader to Refs. [110, 111], and the manuscripts with Hoyle under review, for a more detailed discussion, and for comprehensive citation of the motivating literature, which is beyond the scope of this article.

Throughout we consider a highly viscoelastic filament in which bulk stresses dominate surface tension. We also neglect flow-concentration coupling. Also throughout, the symbol $\sigma_{\rm E}$ denotes the true (and in general time-evolving) tensile stress (the time-evolving tensile force divided by the time-evolving cross sectional area of the filament). It does not denote the so-called engineering tensile stress, which is simply the tensile force divided by the (constant) initial cross sectional area of the filament as measured at the start of the run.

By analogy with our discussion of shear banding above, a useful underpinning concept is that of the stationary homogeneous constitutive relation between the tensile

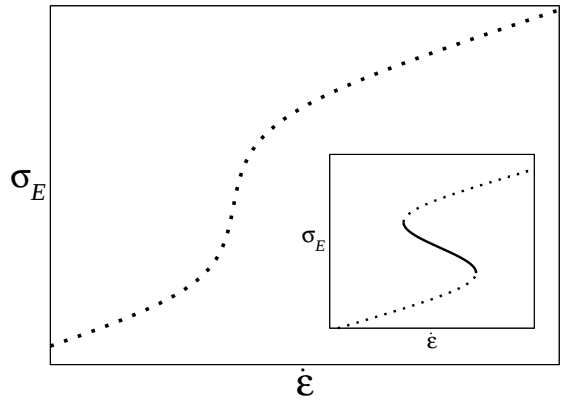

FIG. 8. Underlying stationary constitutive relation between tensile stress and Hencky strain rate, calculated within the assumption of a homogeneous extensional flow. A state of initially homogeneous extensional flow is linearly unstable, in the regime of positive constitutive slope, to the formation of a neck. As described in the text, this result also determines the necking dynamics following the imposition of a tensile stress. Solid line denotes stability; dotted line denotes instability.

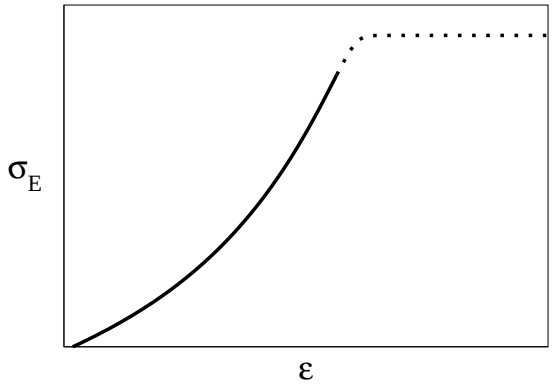

FIG. 9. Typical evolution of the tensile stress following the switch-on of a constant Hencky strain rate. The regime of linear instability to necking is shown as dotted.

stress $\sigma_{\rm E}$ and the Hencky strain rate $\dot{\epsilon}$, calculated by (artificially) assuming that a filament can attain a state in which the stress and strain rate are linked by this time-independent relation, with all the flow variables remaining homogeneous along the filament. Performing a linear stability analysis (at the level of a slender filament approximation) for the dynamics of small heterogeneous perturbations about an initially homogeneous and stationary state on this constitutive curve, with the wavevector of the perturbations along the length of the filament, then reveals instability to necking in any regime where this constitutive curve has positive slope

$$\frac{d\sigma_{\rm E}}{d\dot{\epsilon}} > 0. \tag{5}$$

This tells us that a state of initially homogeneous extensional flow, in which the filament is drawing out and thinning in a uniform way along its length, cannot be maintained in any regime where the underlying extensional constitutive curve is positively sloping. See Fig. 8. Given that most materials indeed have a positively sloping extensional constitutive curve, this suggests that most materials will neck when stretched, which is indeed consistent with experience. An interesting prediction, however, is that of stability against necking in any regime of negative extensional constitutive slope. See the inset of Fig. 8. Note the stark contrast to the corresponding result for shear banding, in which instability is predicted for negative constitutive slope, Eqn. 1.

While the calculation just discussed provides useful intuition, in practice it is not usually possible to prepare a filament in a state of steady uniform extensional flow on the constitutive curve because such a flow is usually unstable, as just shown. In practice one must compute the stability properties of a filament in which stretching was recently commenced. We therefore now consider in turn the three common protocols of step tensile stress, step tensile force, and startup of constant Hencky strain rate. The results that we shall discuss were obtained in analytical calculations performed within highly generalised constitutive descriptions, and confirmed numerically in several models of polymer dynamics [112] (the Oldroyd B, Giesekus, fene-CR, Rolie-poly [72] and pom-pom [113] models), and in tensorial versions of the soft glassy rheology and fluidity models of soft glasses [111].

A. Step stress

We consider first a filament subject at some time $t = 0$ to the switch-on of a constant tensile stress $\sigma_{\rm E}$, which is held constant thereafter. (For times $t < 0$ the sample was undeformed with all internal stresses well relaxed.) In this case, calculations in the polymer models listed above show that the strain rate quickly attains its steady state value on the extensional constitutive curve before any appreciable necking develops. The criterion

$$\frac{d\sigma_{\rm E}}{d\dot{\epsilon}} > 0 \tag{6}$$

for necking thereafter then applies, as sketched in Fig. 8.

B. Step force

Consider now a filament subject at some time $t = 0$ to the switch-on of a constant tensile force F, which is held constant thereafter. In this protocol, typically, the sample attains a state of flow on the underlying homogeneous constitutive curve, then progressively sweeps up this curve as the stress necessarily increases in time to maintain constant force as the cross sectional area thins. The criterion 6 for the onset of necking then applies to good approximation.

C. Constant Hencky strain rate

We consider finally the case of a filament that is initially at rest and with any residual stresses well relaxed, subject at some time $t = 0$ to the switch-on of a Hencky strain rate to some value $\dot{\epsilon}$ that is held constant thereafter. (By this we mean that the nominal Hencky strain rate as averaged along the filament is held constant. Once necking arises, the true Hencky strain rate will vary along the filament's length. As long as the filament remains uniform, however, these nominal and true rates coincide.) Measured in response is the tensile stress startup signal $\sigma_{\rm E}(t)$ as a function of the time t (or accumulated strain $\epsilon = \dot{\epsilon}t$) since the inception of the flow. In Ref. [110] we showed in the polymer models listed above that the filament will be unstable to necking if

$$\frac{d^2\sigma_{\rm E}}{d\epsilon^2} < 0, \tag{7}$$

that is, if the tensile stress shows downward curvature as a function of the accumulated Hencky strain. See Fig. 9.

In some models (the Rolie-poly model without chain stretch, the pom-pom model with saturating chain stretch, and the SGR and fluidity models) an additional mode of instability is possible, given by

$$\frac{dF_{\rm el}}{d\epsilon} < 0. \tag{8}$$

(Indeed this mode can also arise, relatively rarely, under conditions of constant imposed tensile stress or tensile force.) This derivative needs careful interpretation. It is calculated by evolving the full dynamics of any model up to some strain ϵ, then in the next increment of strain over which the derivative of the tensile force F is calculated, disabling the model's relaxational dynamics and evolving only the elastic loading terms. As far as we are aware, this is the closest counterpart in viscoelastic materials of the original Considère criterion, $dF/d\epsilon < 0$, for necking in solids [114]. It is important to note, however, that (8) does not coincide with the original Considère criterion, which in general fails to correctly predict the onset of the necking instability. Indeed it is unclear whether it is possible to access the elastic derivative of (8) experimentally apart from in the limit of infinite extension rate, where relaxational dynamics become unimportant and (8) simply coincides with the original Considère criterion. (In polymer models the onset of this mode also appears related to the presence of a very flat region in the underlying constitutive curve at the strain rate in question, although more work is needed to explore this suggestion fully.) Necking in the elastic limit of viscoelastic models was also discussed in [115].

It is hoped that the criteria just summarised will provide a useful field-guide to the onset of necking instability in filament stretching. A fuller discussion of them can be found in Refs. [110, 111], together with the manuscripts with Hoyle currently under review.

Acknowledgements The author thanks Katherine Carter, Mike Cates, John Girkin, David Hoyle, Robyn Moorcroft, Peter Olmsted and Rangarajan Radhakrishnan for enjoyable collaboration on these topics; and Gareth McKinley, for suggesting the necking calculation to her. Thanks are due to all these, and to Thibaut Divoux, for a critical reading of the manuscript. The author thanks Katherine Carter for assistance in preparing Fig. 6, and Ewan Hemingway for assistance in preparing Fig. 7. Funding of the research leading to these results was provided by the UK's EPSRC (EP/E5336X/1); and the European Research Council under the European Union's Seventh Framework Programme (FP/2007-2013), ERC grant agreement number 279365.

S.M.F. dedicates this manuscript to the memory of Professor Alexei E. Likhtman.

[1] J. Goveas and P. Olmsted, European Physical Journal E **6**, 79 (2001).
[2] P. D. Olmsted, Rheologica Acta **47**, 283 (2008).
[3] M. M. Britton and P. T. Callaghan, Phys. Rev. Lett. **78**, 4930 (1997).
[4] J.-B. Salmon, S. Manneville, and A. Colin, Phys. Rev. E **68**, 051503 (2003).
[5] S. Manneville, A. Colin, G. Waton, and F. Schosseler, Phys. Rev. E **75**, 061502 (2007).
[6] S. Rogers, D. Vlassopoulos, and P. Callaghan, Physical Review Letters **100**, 128304 (2008).
[7] T. Divoux, D. Tamarii, C. Barentin, and S. Manneville, Physical Review Letters **104**, 208301 (2010).
[8] J. D. Martin and Y. T. Hu, Soft Matter **8**, 6940 (2012).
[9] P. Coussot, J. S. Raynaud, F. Bertrand, P. Moucheront, J. P. Guilbaud, H. T. Huynh, S. Jarny, and D. Lesueur, Phys. Rev. Lett. **88**, 218301 (2002).
[10] Y. Li, M. Hu, G. B. McKenna, C. J. Dimitriou, G. H. McKinley, R. M. Mick, D. C. Venerus, and L. A. Archer, Journal of Rheology **57**, 1411 (2013).
[11] S.-Q. Wang, G. Liu, S. Cheng, P. E. Boukany, Y. Wang, and X. Li, Journal of Rheology **58**, 1059 (2014).
[12] S.-Q. Wang, S. Ravindranath, and P. E. Boukany, Macromolecules **44**, 183 (2011).
[13] S. Ravindranath, S.-Q. Wang, M. Ofechnowicz, and R. P. Quirk, Macromolecules **41**, 2663 (2008).
[14] T. Divoux, M. A. Fardin, S. Manneville, and S. Lerouge, Annual Review of Fluid Mechanics **48**, 81 (2016).
[15] S. Manneville, Rheologica Acta **47**, 301 (2008).
[16] S. M. Fielding, Reports on Progress in Physics **77**, 102601 (2014).
[17] R. L. Moorcroft and S. M. Fielding, Physical Review Letters **110**, 086001 (2013).
[18] R. L. Moorcroft and S. M. Fielding, Journal of Rheology

58, 103 (2014).
[19] J. M. Adams and P. D. Olmsted, Physical Review Letters **102**, 067801 (2009).
[20] R. L. Moorcroft, M. E. Cates, and S. M. Fielding, Physical Review Letters **106**, 055502 (2011).
[21] M. L. Manning, J. S. Langer, and J. M. Carlson, Phys. Rev. E **76**, 056106 (2007).
[22] M. L. Manning, E. G. Daub, J. S. Langer, and J. M. Carlson, Phys. Rev. E **79**, 016110 (2009).
[23] E. A. Jagla, Journal of Statistical Mechanics - Theory and Experiment P12025 (2010).
[24] J. M. Adams, S. M. Fielding, and P. D. Olmsted, Journal of Rheology **55**, 1007 (2011).
[25] P. E. Boukany and S.-Q. Wang, Macromolecules **41**, 1455 (2008).
[26] Y. T. Hu, C. Palla, and A. Lips, Journal of Rheology **52**, 379 (2008).
[27] P. E. Boukany and S.-Q. Wang, Journal of Rheology **53**, 73 (2009).
[28] Y. Hu, L. Wilen, A. Philips, and A. Lips, Journal of Rheology **51**, 275 (2007).
[29] P. E. Boukany and S.-Q. Wang, Soft Matter **5**, 780 (2009).
[30] T. Divoux, C. Barentin, and S. Manneville, Soft Matter **7**, 9335 (2011).
[31] J. D. Martin and Y. T. Hu, Soft Matter **8**, 6940 (2012).
[32] J. Cao and A. E. Likhtman, Phys. Rev. Lett. **108**, 028302 (2012).
[33] Y. Shi, M. B. Katz, H. Li, and M. L. Falk, Physical Review Letters **98**, 185505 (2007).
[34] S. M. Fielding, R. L. Moorcroft, R. G. Larson, and M. E. Cates, Journal of Chemical Physics **138**, 12A504 (2013).
[35] A. Kurokawa, V. Vidal, K. Kurita, T. Divoux, and S. Manneville, Soft Matter **11**, 9026 (2015).
[36] P. E. Boukany and S.-Q. Wang, Macromolecules **41**, 1455 (2008).
[37] Y. T. Hu and A. Lips, Journal of Rheology **49**, 1001 (2005).
[38] Y. T. Hu, Journal of Rheology **54**, 1307 (2010).
[39] T. Divoux, C. Barentin, and S. Manneville, Soft Matter **7**, 8409 (2011).
[40] T. Gibaud, D. Frelat, and S. Manneville, Soft Matter **6**, 3482 (2010).
[41] K. Hyun, M. Wilhelm, C. O. Klein, K. S. Cho, J. G. Nam, K. H. Ahn, S. J. Lee, R. H. Ewoldt, and G. H. McKinley, Progress in Polymer Science **36**, 1697 (2011).
[42] K. A. Carter, J. M. Girkin and S. M. Fielding, http://arxiv.org/abs/1510.00191. Shear banding in large amplitude oscillatory shear (LAOStrain and LAOStress)of polymers and wormlike micelles, J. Rheol. 60, XX-XX (2016).
[43] J. Yerushalmi, S. Katz, and R. Shinnar, Chemical Engineering Science **25**, 1891 (1970).
[44] N. A. Spenley, M. E. Cates, and T. C. B. McLeish, Phys. Rev. Lett. **71**, 939 (1993).
[45] P. Olmsted, O. Radulescu, and C. Lu, Journal of Rheology **44**, 257 (2000).
[46] C. Grand, J. Arrault, and M. Cates, Journal de Physique II **7**, 1071 (1997).
[47] V. Schmitt, C. M. Marques, and F. Lequeux, Phys. Rev. **E52**, 4009 (1995).
[48] F. Brochard and P. G. Degennes, Macromolecules **10**, 1157 (1977).
[49] E. Helfand and G. H. Fredrickson, Phys. Rev. Lett. **62**, 2468 (1989).
[50] M. Doi and A. Onuki, J. Phys. II (France) **2**, 1631 (1992).
[51] S. T. Milner, Phys. Rev. **E 48**, 3674 (1993).
[52] X. L. Wu, D. J. Pine, and P. K. Dixon, Phys. Rev. Lett. **66**, 2408 (1991).
[53] A. N. Beris and V. G. Mavrantzas, J. Rheol. **38**, 1235 (1994).
[54] T. Sun, A. C. Balazs, and D. Jasnow, Phys. Rev. **E 55**, R6344 (1997).
[55] S. Fielding and P. Olmsted, Physical Review E **68**, 036313 (2003).
[56] S. Fielding and P. Olmsted, Physical Review Letters **90**, 224501 (2003).
[57] S. Fielding and P. Olmsted, European Physical Journal E **11**, 65 (2003).
[58] M. Cromer, M. C. Villet, G. H. Fredrickson, and L. G. Leal, Physics of Fluids **25**, 051703 (2013).
[59] M. Cromer, G. H. Fredrickson, and L. G. Leal, Physics of Fluids **26**, 063101 (2014).
[60] R. Besseling, L. Isa, P. Ballesta, G. Petekidis, M. E. Cates, and W. C. K. Poon, Physical Review Letters **105**, 268301 (2010).
[61] H. Jin, K. Kang, K. H. Ahn, and J. K. G. Dhont, Soft Matter **10**, 9470 (2014).
[62] A. Ragouilliaux, B. Herzhaft, F. Bertrand, and P. Coussot, Rheologica Acta **46**, 261 (2006).
[63] R. Bandyopadhyay, G. Basappa, and A. K. Sood, Phys. Rev. Lett. **84**, 2022 (2000).
[64] R. Ganapathy and A. K. Sood, Phys. Rev. Lett. **96**, 108301 (2006).
[65] S. Fielding and P. Olmsted, Physical Review Letters **92**, 084502 (2004).
[66] A. Aradian and M. Cates, Europhysics Letters **70**, 397 (2005).
[67] A. Aradian and M. E. Cates, Phys. Rev. E **73**, 041508 (2006).
[68] C. Derec, G. Ducouret, A. Ajdari, and F. Lequeux, Phys. Rev. E **67**, 061403 (2003).
[69] S. A. Rogers, P. T. Callaghan, G. Petekidis, and D. Vlassopoulos, J. Rheology **54**, 133 (2010).
[70] N. Koumakis and G. Petekidis, Soft Matter **7**, 2456 (2011).
[71] C. J. Dimitriou and G. H. McKinley, Soft Matter **10**, 6619 (2014).
[72] A. E. Likhtman and R. S. Graham, J. Non-Newt. Fl. Mech. **114**, 1 (2003).
[73] T. Gibaud, C. Barentin, and S. Manneville, Physical Review Letters **101**, 258302 (2008).
[74] M. Mohagheghi and B. Khomami, Elucidating the flow-microstructure coupling in entangled polymer melts: part II. Molecular mechanisms of shear banding. J. Rheol. 60, XX-XX (2016).
[75] J. Colombo and E. Del Gado, Journal of Rheology **58**, 1089 (2014).
[76] F. Varnik, L. Bocquet, and J. L. Barrat, J. Chem. Phys. **120**, 2788 (2004).
[77] G. P. Shrivastav, P. Chaudhuri, and J. Horbach, Heterogeneous dynamics during yielding of glasses: effect of aging, J. Rheol. 60, XX-XX (2016).
[78] A. Kabla, J. Scheibert, and G. Debregeas, Journal of Fluid Mechanics **587**, 45 (2007).
[79] J. D. Barry, D. Weaire, and S. Hutzler, Rheologica Acta **49**, 687 (2010), 5th Annual European Rheology Confer-

ence (AERC 2009), Cardiff Univ, Cardiff, Wales, Apr 15-17, 2009.
[80] A. Lehtinen, A. Puisto, X. Illa, M. Mohtaschemi, and M. J. Alava, Soft Matter **9**, 8041 (2013).
[81] A. R. Hinkle and M. R. Falk, A Small-gap Effective-Temperature Model of Transient Shear Band Formation During Flow, J. Rheol. 60, XX-XX (2016).
[82] T. Divoux, V. Grenard, and S. Manneville, Physical Review Letters **110**, 018304 (2013).
[83] A. Magnin and J. Piau, Journal of Non-Newtonian Fluid Mechanics **36**, 85 (1990).
[84] V. Grenard, T. Divoux, N. Taberlet, and S. Manneville, Soft Matter **10**, 1555 (2014).
[85] T. Sentjabrskaja, P. Chaudhuri, M. Hermes, W. C. K. Poon, J. Horbach, S. U. Egelhaaf, and M. Laurati, Scientific Reports **5**, 11884 (2015).
[86] P. Chaudhuri and J. Horbach, Physical Review E **88**, 040301 (2013).
[87] O. S. Agimelen and P. D. Olmsted, Physical Review Letters **110**, 204503 (2013).
[88] G. Marrucci, Journal of Non-Newtonian Fluid Mechanics **62**, 279 (1996).
[89] G. Ianniruberto and G. Marrucci, Journal of Rheology **58**, 89 (2014).
[90] G. Marrucci and N. Grizzuti, Journal of Rheology **27**, 433 (1983).
[91] X. Li and S.-Q. Wang, Rheologica Acta **49**, 985 (2010).
[92] P. E. Boukany and S.-Q. Wang, Macromolecules **42**, 2222 (2009).
[93] S.-Q. Wang, S. Ravindranath, P. Boukany, M. Olechnowicz, R. P. Quirk, A. Halasa, and J. Mays, Phys. Rev. Lett. **97**, 187801 (2006).
[94] S. Ravindranath and S.-Q. Wang, Macromolecules **40**, 8031 (2007).
[95] Y. Fang, G. Wang, N. Tian, X. Wang, X. Zhu, P. Lin, G. Ma, and L. Li, Journal of Rheology **55**, 939 (2011).
[96] L. A. Archer, Y.-L. Chen, and R. G. Larson, Journal of Rheology **39**, 519 (1995).
[97] S. Ravindranath, S.-Q. Wang, M. Olechnowicz, V. S. Chavan, and R. P. Quirk, Rheologica Acta **50**, 97 (2011).
[98] P. E. Boukany, S.-Q. Wang, and X. Wang, Macromolecules **42**, 6261 (2009).
[99] L. Zhou, L. P. Cook, and G. H. McKinley, Journal of Non-Newtonian Fluid Mechanics **165**, 1462 (2010).
[100] L. Zhou, R. H. Ewoldt, L. P. Cook, and G. H. McKinley, in *XVTH International Congress on Rheology - The Society of Rheology 80th Annual Meeting, Pts 1 and 2*, Vol. 1027 of *AIP Conference Proceedings*, edited by A. Co, L. Leal, R. Colby, and A. Giacomin (PUBLISHER, ADDRESS, 2008), pp. 189–191, 15th International Congress on Rheology/80th Annual Meeting of the Society-of-Rheology, Monterey, CA, AUG 03-08, 2008.
[101] P. Tapadia, S. Ravindranath, and S. Q. Wang, Phys. Rev. Lett. **96**, 196001 (2006).
[102] I. Cohen, B. Davidovitch, A. B. Schofield, M. P. Brenner, and D. A. Weitz, Physical Review Letters **97**, 215502 (2006).
[103] C. Perge, N. Taberlet, T. Gibaud, and S. Manneville, Journal of Rheology **58**, 1331 (2014).
[104] T. Gibaud, C. Perge, S. B. Lindstrom, N. Taberlet, and S. Manneville, Soft Matter **12**, 1701 (2016).
[105] F. Rouyer, S. Cohen-Addad, R. Hoehler, and et al., European Physical Journal E **27**, 309 (2008).
[106] Y. Guo, W. Yu, Y. Xu, and C. Zhou, Soft Matter **7**, 2433 (2011).
[107] C. J. Dimitriou, L. Casanellas, T. J. Ober, and G. H. McKinley, Rheologica Acta **51**, 395 (2012).
[108] A. K. Gurnon and N. J. Wagner, Journal of Rheology **56**, 333 (2012).
[109] M. A. Calabrese and S. A. Rogers, L. Porcar and N. J. Wagner, Understanding steady and dynamic shear banding in a wormlike micellar solution. J. Rheol. 60, XX-XX (2016).
[110] S. M. Fielding, Phys. Rev. Lett. **107**, 258301 (2011).
[111] D. M. Hoyle and S. M. Fielding, Physical Review Letters **114**, 158301 (2015).
[112] R. Larson, *Constitutive Equations for Polymer Melts and Solutions* (Butterwirth Publishers, Stoneham, MA, 1988).
[113] T. C. B. McLeish and R. G. Larson, J. Rheol. **42**, 81 (1998).
[114] M. Considère, Ann. Ponts Chausées **9**, 574 (1885).
[115] O. Hassager, M. I. Kolte, and M. Renardy, Journal of Non-Newtonian Fluid Mechanics **76**, 137 (1998).